Therefore, *DNYC1H1* may have broad biological effects on development and maintenance of the nervous system.

In this study, we describe a family containing three individuals with dominant spinal muscular atrophy with lower extremity predominance. Exome sequencing identified an identical *DYNC1H1* mutation found in a pedigree with axonal CMT [2], demonstrating the pleotropic effects of the *DYNC1H1* mutation.

Subjects and methods

Subjects

Patient 1 This female patient was born after 41 weeks of gestation. Pregnancy was uneventful. Birth weight was 3,080 g. Her initial development was normal, and head control was recognized at 3–4 months. Late infantile motor development was mildly delayed, and she could walk unassisted at 1 year and 8 months. Unstable gait persisted thereafter, and she was referred to us at 3 years and 1 month of age for evaluation. On examination, proximal lower limb-dominant muscle atrophy and decreased deep tendon reflex were noted. Gower's sign was positive. No other neurological deficits were demonstrated. No sensory disturbance or ataxia was present.

The following examinations were performed at 3 years and 1 month of age. Neither serum transaminase nor creatine kinase was elevated. Motor nerve conduction velocity was within the normal limits (55.8 m/s for the right tibial nerve). Brain MRI revealed normal findings. Muscle computed tomography (CT) demonstrated severe atrophy and lipid degeneration, predominantly in the bilateral quadriceps femoris muscle (Fig. 1). The upper limbs and distal lower limbs were not affected. A muscle biopsy from the quadriceps femoris muscle demonstrated severe grouping atrophy of type 2 fibers with a massive increase in the amount of fibrous tissue and sparse enlarged type 1 fibers (Fig. 2).

The patient is currently 18 years old and graduated from regular high school. Her motor development has steadily progressed, and she only shows moderate proximal lower limb-dominant muscle weakness and atrophy. She can walk unassisted and shows a waddling gait and positive Gower's sign. No sensory disturbance or ataxia is noted. She does not have any intellectual disability.

Patient 2 Patient 2 is the half brother of patient 1. He was born after 38 weeks of gestation to the same mother and a different father from patient 1's. His birth weight was 2,405 g. He could control his head at 3–4 months, turn over at 6 months, and sit unassisted at 7–8 months. His motor development was delayed thereafter, and he walked unassisted at 1 year and 7 months. His mental development was normal. Because of a persistently unstable gait, he was hospitalized and examined at 5 years and 11 months. Physical examination revealed moderate muscle weakness in the proximal lower limb, but Gower's sign was negative. Deep tendon reflex was normal. No sensory disturbance or ataxia was recognized. Ankle joint contracture and foot deformity were absent.

The following examinations were performed at 5 years and 11 months of age. Serum transaminase and creatine kinase levels were normal. Brain and spinal MRI revealed no abnormal findings. Motor nerve conduction velocity and amplitude were within the normal limits (51.1 m/s, 4.6 mV for the right median nerve, 51.1 m/s, 9.9 mV for the right tibial nerve). Sensory nerve conduction velocity and amplitude were also within the normal limits (57.3 m/s, 28.4 uV for the right median nerve, 63.7 m/s, 9.6 uV for the right sural nerve). Needle electromyography of the anterior tibial muscle showed long high-amplitude discharges (3.5–4.0 mV, 10 ms) consistent with a neurogenic pattern, although no denervation potential, including positive sharp wave or fibrillation potential, was present, while the right biceps brachii showed inconclusive results. Muscle CT revealed severe atrophy and lipid degeneration, most predominantly in the bilateral quadriceps femoris. The upper limbs and distal lower limbs were not affected (Fig. 1).

The patient is now 12 years old and can walk unassisted but with a waddling gait. He has shown no further deterioration of motor function. Proximal lower limb weakness and wasting are evident, but the patient shows no upper limb weakness. No sensory disturbance or ataxia has been recognized.

Patient 3 Patient 3 is the mother of the two sibs. She is currently 50 years of age. No family history (except for her children) of neuromuscular disorders was noted. Until we examined the second sib, she had not been noted to have proximal lower limb muscle weakness. She did not recall her infantile development, and it was impossible to obtain further information. She graduated from a regular high school, married, and raised her children. She has not shown any neurological deterioration. She did not show a waddling gait, but had difficulty squatting. She was examined at 44 years of age. Her deep tendon reflex was normal, and no ankle joint contracture was present. Muscle CT revealed bilateral quadriceps-dominant muscle atrophy and lipid degeneration (Fig. 1). She also demonstrated mild muscle atrophy in her hip. Unfortunately, CT of the distal lower limb muscle could not be performed.

Exome sequencing

We performed the whole-exome sequencing of two patients (II-1 and II-2; Fig. 3a). Three micrograms of genomic DNA

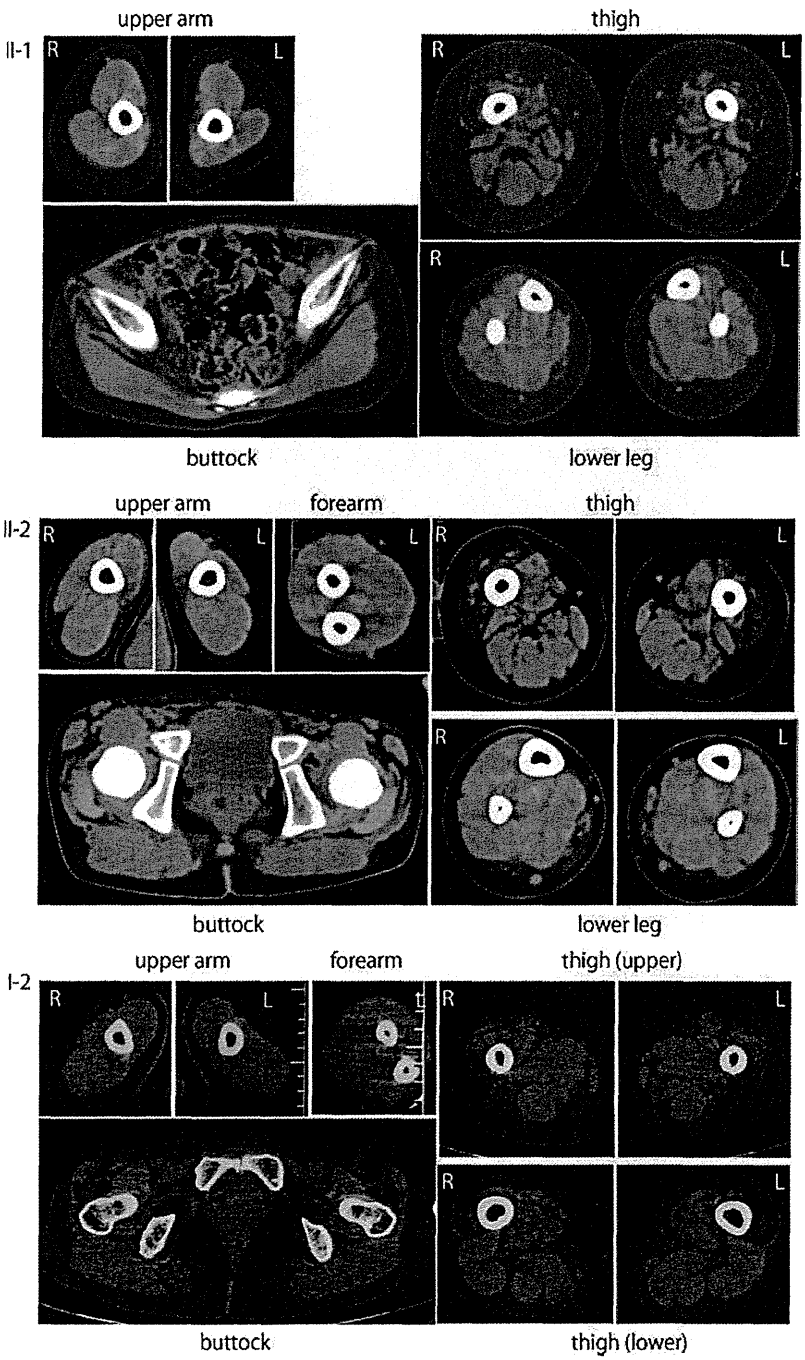

Fig. 1 Muscle imaging. Muscle computed tomography images of patient II-1 at the age of 3 years and 1 month (*upper*), patient II-2 at the age of 5 years and 11 months (*middle*), and patient I-1 at the age of 44 years (*lower*) are displayed. *R* right, *L* left

was processed using a SureSelect Human All Exon Kit v.1 (approximately 180,000 exons covering 38 Mb of the CCDS database) (Agilent Technologies, Santa Clara, CA) according to the manufacturer's protocol. Captured DNA was diluted to a concentration of 8 pM and sequenced on a Genome Analyzer IIx (Illumina, San Diego, CA) with 76-bp paired-end reads. We used two of the eight lanes in the flow cell (Illumina). Image analyses and base calling were performed by sequence control software real-time analysis and/or Off-line Basecaller software v1.6.0 (Illumina). Alignment was performed using CASAVA software v1.6.0. The quality-controlled (Path Filter) reads were mapped to the human reference genome (UCSC hg19, NCBI build 37), using mapping and assembly with quality (MAQ) and NextGENe software v2.0 (SoftGenetics, State College, PA). SNPs in MAQ-passed reads were annotated using the

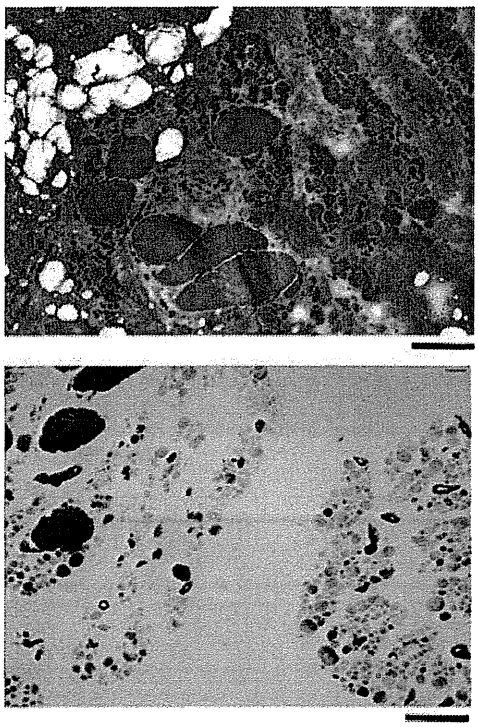

Fig. 2 Histological study. Hematoxylin–eosin staining (*upper*) and ATPase staining (pH=4.6, *lower*) of the quadriceps femoris muscle of patient II-1. The *scale bar* indicates 100 μm in length

SeattleSeq Annotation website (http://gvs.gs.washington.edu/SeattleSeqAnnotation/).

Priority scheme and capillary sequencing

We adopted a prioritization scheme used in recent studies to identify the pathogenic mutation [5–7]. Called variants found by each informatics method filtered into unregistered variants (excluding registered dbSNP131 and 1,000 genomes), overlapping variants called in common by NextGENe and MAQ, nonsynonymous changes (NS), splice site mutations (±2 bp from the exon–intron junctions) (SS), small insertions or deletions (indels), and overlapping variants called in II-1 and II-2 were checked, and variants found in our 33 in-house exomes derived from 19 healthy individuals and 14 individuals with unrelated diseases were excluded (Table 1). An online human genome mutation database (HGMD, https://portal.biobase-international.com/hgmd/pro/start.php) was referred to as a reference for disease-causing mutations. The variants were confirmed as true positives by Sanger sequencing of polymerase chain reaction products amplified using genomic DNA as a template. Sanger sequencing was performed on an ABI3500XL or ABI3100 autosequencer (Life Technologies, Carlsbad, CA). Sequencing data were analyzed using Sequencer software (Gene Codes Corporation, Ann Arbor, MI).

A total of 177 Japanese control samples (354 alleles) were check by high-resolution melting analysis using a LightCycler 480 (Roche Diagnostics, Otsu, Japan) to see the variant frequency. The reaction was performed in 10 μl containing 10 ng of genomic DNA, 0.2 mM dNTPs,

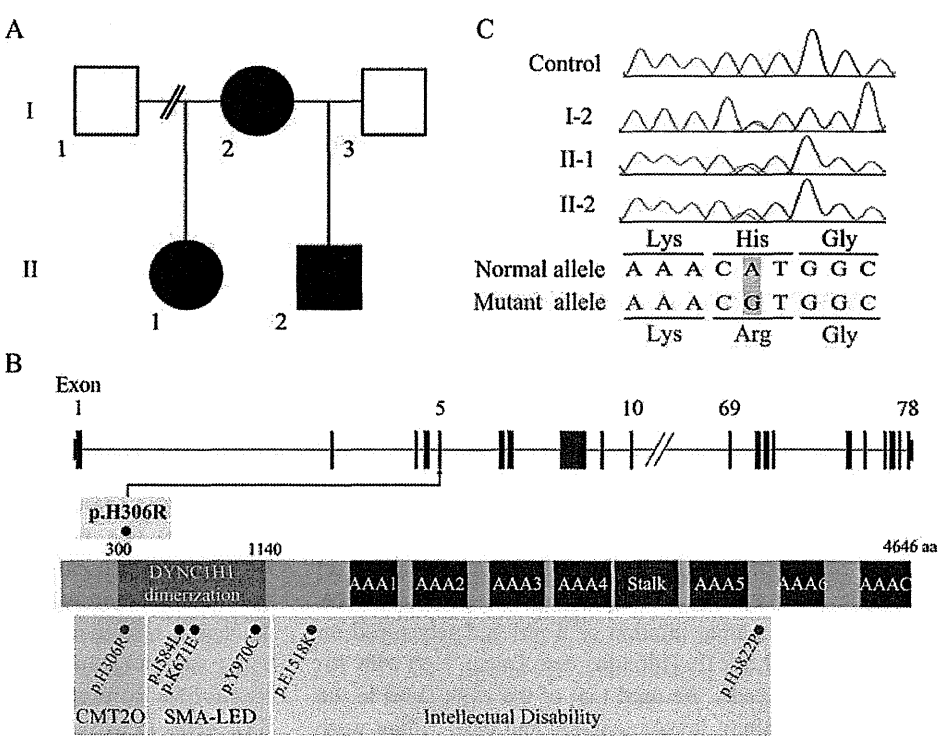

Fig. 3 Genetic study. **a** Familial pedigree. **b** The gene structure of *DYNC1H1* with the mutation [p.H306R (c.917A>G)] (*upper*), the protein structure with functional domains (*middle*), and reported mutations corresponding to respective diseases (*lower*). *AAA* ATPase domains (AAA 1 to 6), *AAAC* unrelated seventh domain. **c** Sequences of a control and the family members are displayed. Heterozygous mutations are observed in patients I-2, II-1, and II-2

Table 1 Variant priority scheme of exome sequencing data

	Half sister		Half brother	
	NextGENe	MAQ (SeattleSeq)	NextGENe	MAQ (SeattleSeq)
Total variants called	73,966	174,757	73,370	163,707
Autosomal+chr X	71,522	174,165	70,068	163,013
Unknown SNP variants (dbSNP, 1,000 genomes)	11,132	21,284	10,857	19,858
Overlap of NextGENe and MAQ	1,598		1,482	
NS/SS/I	426		411	
Overlapping in half sibs	135			
Unknown variants (in-house database)	62			

MAQs were annotated using SeattleSeq annotation. The annotation includes gene names, dbSNP rs IDs, and SNP functions (e.g., missense), protein positions and amino acid changes. *NS* nonsynonymous, *SS* splice site (±2 bp), *I* indels

0.125 U of ExTaq (Takara Bio, Inc., Otsu, Japan), 1× buffer, and 1.5 μM SYTO9 (Invitrogen, Carlsbad, CA).

Results

Approximately 9.8 and 9.5 Gb of sequence data were generated for II-1 and II-2, respectively. This approach resulted in more than 85.8 % (II-1) and 86.5 % (II-2) of the target regions being covered by ten reads or more. Two informatics methods identified 62 potentially pathogenic changes (Table 1). We found a missense mutation [p.H306R (c.917A>G)] in *DYNC1H1* from among 62 variants using the HGMD as a reference; this mutation has been reported as a causative mutation for CMT disease [2]. The heterozygous missense mutation was confirmed in I-2, II-1, and II-2 (Fig. 3b). This missense mutation was not found in 177 control samples.

Discussion

The identical *DYNC1H1* mutation (p.H306R) found in a large pedigree with axonal type of CMT disease was detected by exome sequencing in a family with a unique form of quadriceps-dominant neurogenic muscular atrophy [2]. Three members of the family demonstrated very similar clinical features, which were distinct from CMT disease. The most striking feature was a unique distribution of muscle involvement. The quadriceps femoris muscle was almost selectively involved in the early course of the disease, and the proximal lower limb was predominantly involved throughout the disease course. Recently, three other missense mutations were detected in families with SMA-LED. Clinical features of the current family are essentially consistent with those of SMA-LED, hallmarks of which are early childhood onset of proximal leg weakness with muscle atrophy and nonlength-dependent motor neuron disease without sensory involvement [3]. Nonprogressive clinical course despite early childhood onset as in our family should be another hallmark of SMA-LED. These cumulative data clearly indicate that *DYNC1H1* plays an essential role in maintenance of spinal motor neurons and their axon.

Thus far, four missense mutations (p.H306R, p.I584L, p.K671E, p.Y970C) identified in human cases of CMT or SMA-LED are located in the same tail domain for DYNC1H1 dimerization. It is of note that three missense mutations (p.F580Y, p.G1042A, p.T1057C) found in mouse models are also located in the tail domain [8–10]. These mice involve not only spinal motor neurons but also sensory and cortical neurons. The tail domain is thought to be essential for dimerization of dynein heavy chains, and thus, missense mutations in the tail domain may disrupt function of dynein complex formation in a dominant negative manner. Two distinct de novo mutations (p.E1518K, p.H3822P) identified in patients with severe intellectual disability and variable neuronal migration defects were located outside of the tail domain. These patients also showed possible peripheral nerve involvement, but formal neurophysiological investigation was not available. Since mice with *Dync1h1* abnormality show broad central nervous system involvement, *DNYC1H1* is likely to cause a wide range of neuronal migration disorders.

CMT disease with the p.H306R mutation has been designated as CMT2O (OMIM 614228). Most members of the pedigree with p.H306R reported by Weedon et al. demonstrated distal dominant muscle weakness, while one patient showed proximal lower limb-dominant muscle atrophy as in our family [2]. Therefore, the same missense mutation in the tail domain could cause CMT2O phenotype and SMA-LED phenotype even within the same pedigree. It is hard to explain the underlying mechanism of pleotropic effects of the mutation. Further studies are absolutely necessary to elucidate phenotype–genotype correlation and pleiotropic mutational consequences.

Acknowledgments We would like to thank the family for their participation in this study. This work was supported by research grants from the Ministry of Health, Labour and Welfare (H.S., N. Miyake, and

N. Matsumoto); a Grant-in-Aid for Scientific Research from the Japan Society for the Promotion of Science (N. Miyake and N. Matsumoto); a grant from the Japan Science and Technology Agency (N. Matsumoto), the Strategic Research Program for Brain Sciences (N. Matsumoto); a Grant-in-Aid for Scientific Research on Innovative Areas (Foundation of Synapse and Neurocircuit Pathology) from the Ministry of Education, Culture, Sports, Science and Technology of Japan (N. Matsumoto); a research grant from Naito Foundation (N. Matsumoto); and research grants from Takeda Science Foundation (N. Miyake and N. Matsumoto). This work was performed at the Advanced Medical Research Center, Yokohama City University, Japan.

References

1. Pfister KK, Shah PR, Hummerich H, Russ A, Cotton J, Annuar AA, King SM, Fisher EM (2006) Genetic analysis of the cytoplasmic dynein subunit families. PLoS Genet 2(1):e1. doi:10.1371/journal.pgen.0020001
2. Weedon MN, Hastings R, Caswell R, Xie W, Paszkiewicz K, Antoniadi T, Williams M, King C, Greenhalgh L, Newbury-Ecob R, Ellard S (2011) Exome sequencing identifies a DYNC1H1 mutation in a large pedigree with dominant axonal Charcot–Marie–Tooth disease. Am J Hum Genet 89(2):308–312. doi:10.1016/j.ajhg.2011.07.002
3. Harms MB, Ori-McKenney KM, Scoto M, Tuck EP, Bell S, Ma D, Masi S, Allred P, Al-Lozi M, Reilly MM, Miller LJ, Jani-Acsadi A, Pestronk A, Shy ME, Muntoni F, Vallee RB, Baloh RH (2012) Mutations in the tail domain of DYNC1H1 cause dominant spinal muscular atrophy. Neurology 78(22):1714–1720. doi:10.1212/WNL.0b013e3182556c05
4. Willemsen MH, Vissers LE, Willemsen MA, van Bon BW, Kroes T, de Ligt J, de Vries BB, Schoots J, Lugtenberg D, Hamel BC, van Bokhoven H, Brunner HG, Veltman JA, Kleefstra T (2012) Mutations in DYNC1H1 cause severe intellectual disability with neuronal migration defects. J Med Genet 49(3):179–183. doi:10.1136/jmedgenet-2011-100542
5. Tsurusaki Y, Okamoto N, Suzuki Y, Doi H, Saitsu H, Miyake N, Matsumoto N (2011) Exome sequencing of two patients in a family with atypical X-linked leukodystrophy. Clin Genet 80 (2):161–166. doi:10.1111/j.1399-0004.2011.01721.x
6. Saitsu H, Osaka H, Sasaki M, Takanashi J, Hamada K, Yamashita A, Shibayama H, Shiina M, Kondo Y, Nishiyama K, Tsurusaki Y, Miyake N, Doi H, Ogata K, Inoue K, Matsumoto N (2011) Mutations in POLR3A and POLR3B encoding RNA polymerase III subunits cause an autosomal-recessive hypomyelinating leukoencephalopathy. Am J Hum Genet 89(5):644–651. doi:10.1016/j.ajhg.2011.10.003
7. Doi H, Yoshida K, Yasuda T, Fukuda M, Fukuda Y, Morita H, Ikeda S, Kato R, Tsurusaki Y, Miyake N, Saitsu H, Sakai H, Miyatake S, Shiina M, Nukina N, Koyano S, Tsuji S, Kuroiwa Y, Matsumoto N (2011) Exome sequencing reveals a homozygous SYT14 mutation in adult-onset, autosomal-recessive spinocerebellar ataxia with psychomotor retardation. Am J Hum Genet 89 (2):320–327. doi:10.1016/j.ajhg.2011.07.012
8. Hafezparast M, Klocke R, Ruhrberg C, Marquardt A, Ahmad-Annuar A, Bowen S, Lalli G, Witherden AS, Hummerich H, Nicholson S, Morgan PJ, Oozageer R, Priestley JV, Averill S, King VR, Ball S, Peters J, Toda T, Yamamoto A, Hiraoka Y, Augustin M, Korthaus D, Wattler S, Wabnitz P, Dickneite C, Lampel S, Boehme F, Peraus G, Popp A, Rudelius M, Schlegel J, Fuchs H, Hrabe de Angelis M, Schiavo G, Shima DT, Russ AP, Stumm G, Martin JE, Fisher EM (2003) Mutations in dynein link motor neuron degeneration to defects in retrograde transport. Science 300(5620):808–812. doi:10.1126/science.1083129
9. Chen XJ, Levedakou EN, Millen KJ, Wollmann RL, Soliven B, Popko B (2007) Proprioceptive sensory neuropathy in mice with a mutation in the cytoplasmic dynein heavy chain 1 gene. J Neurosci 27(52):14515–14524. doi:10.1523/JNEUROSCI.4338-07.2007
10. Ori-McKenney KM, Vallee RB (2011) Neuronal migration defects in the Loa dynein mutant mouse. Neural Dev 6:26. doi:10.1186/1749-8104-6-26

Epilepsia, 53(8):1441–1449, 2012
doi: 10.1111/j.1528-1167.2012.03548.x

FULL-LENGTH ORIGINAL RESEARCH

CASK aberrations in male patients with Ohtahara syndrome and cerebellar hypoplasia

***Hirotomo Saitsu, †Mitsuhiro Kato, ‡Hitoshi Osaka, §Nobuko Moriyama, ¶Hideki Horita, *Kiyomi Nishiyama, *Yuriko Yoneda, *Yukiko Kondo, *Yoshinori Tsurusaki, *Hiroshi Doi, *Noriko Miyake, †Kiyoshi Hayasaka, and *Naomichi Matsumoto**

***Department of Human Genetics, Yokohama City University Graduate School of Medicine, Kanazawa-ku, Yokohama, Japan; †Department of Pediatrics, Yamagata University Faculty of Medicine, Yamagata, Japan; ‡Division of Neurology, Clinical Research Institute, Kanagawa Children's Medical Center, Minami-ku, Yokohama, Japan; §Department of Pediatrics, Hitachi, Ltd., Hitachinaka General Hospital, Hitachinaka, Japan; and ¶Department of Pediatrics, Ibaraki Disabled Children's Hospital, Mito, Japan**

Summary

Purpose: Ohtahara syndrome (OS) is one of the most severe and earliest forms of epilepsy. *STXBP1* and *ARX* mutations have been reported in patients with OS. In this study, we aimed to identify new genes involved in OS by copy number analysis and whole exome sequencing.

Methods: Copy number analysis and whole exome sequencing were performed in 34 and 12 patients with OS, respectively. Fluorescence in situ hybridization, quantitative polymerase chain reaction (PCR), and breakpoint-specific and reverse-transcriptase PCR analyses were performed to characterize a deletion. Immunoblotting using lymphoblastoid cells was done to examine expression of CASK protein.

Key Findings: Genomic microarray analysis revealed a 111-kb deletion involving exon 2 of *CASK* at Xp11.4 in a male patient. The deletion was inherited from his mother, who was somatic mosaic for the deletion. Sequencing of the mutant transcript expressed in lymphoblastoid cell lines derived from the patient confirmed the deletion of exon 2 in the mutant transcript with a premature stop codon. Whole exome sequencing identified another male patient who was harboring a c.1A>G mutation in *CASK*, which occurred de novo. Both patients showed severe cerebellar hypoplasia along with other congenital anomalies such as micrognathia, a high arched palate, and finger anomalies. No CASK protein was detected by immunoblotting in lymphoblastoid cells derived from two patients.

Significance: The detected mutations are highly likely to cause the loss of function of the CASK protein in male individuals. *CASK* mutations have been reported in patients with intellectual disability with microcephaly and pontocerebellar hypoplasia or congenital nystagmus, and those with FG syndrome. Our data expand the clinical spectrum of *CASK* mutations to include OS with cerebellar hypoplasia and congenital anomalies at the most severe end.

KEY WORDS: *CASK*, Ohtahara syndrome, Male, Cerebellar hypoplasia.

Ohtahara syndrome (OS), also known as early infantile epileptic encephalopathy with suppression-burst, is one of the most severe and earliest forms of epilepsy (Ohtahara et al., 1976). It is characterized by early onset of seizures, typically frequent epileptic spasms, seizure intractability, characteristic suppression-burst patterns on electroencephalography (EEG), and poor outcome with severe psychomotor retardation (Djukic et al., 2006; Ohtahara & Yamatogi, 2006). Brain malformations such as cerebral dysgenesis, hemimegalencephaly, Aicardi syndrome, and porencephaly are often associated with OS (Yamatogi & Ohtahara, 2002). However, mutations of the *ARX* and *STXBP1* gene have been reported in individuals with OS who showed no brain malformations, indicating that mutated genes are involved in OS (Kato et al., 2007, 2009; Fullston et al., 2010; Giordano et al., 2010; Saitsu et al., 2008, 2010).

CASK (Genbank accession number NM_003688.3) at Xp11.4 encodes a calcium/calmodulin-dependent serine protein kinase of 921 amino acids belonging to the membrane-associated guanylate kinase protein family (Hsueh, 2006). Accumulating evidence indicates that *CASK* is essential for synapse formation at both presynaptic and postsynaptic junctions. In addition, CASK enters the nucleus and regulates expression of genes involved in cortical development (Hsueh, 2006). Recently, heterozygous loss-of-function mutations in *CASK* were found in four female patients with X-linked intellectual disability (ID);

Accepted April 23, 2012; Early View publication June 18, 2012.
Address correspondence to Hirotomo Saitsu, Department of Human Genetics, Yokohama City University Graduate School of Medicine, 3-9 Fukuura, Kanazawa-ku, Yokohama 236-0004, Japan. E-mail: hsaitsu@yokohama-cu.ac.jp

microcephaly and pontocerebellar hypoplasia (MICPCH) and a hemizygous synonymous c.915G>A mutation, which caused skipping of exon 9 of *CASK* in about 20% of the mutant transcripts, was found in a male patient with the same disease and presentation (Najm et al., 2008). To date, 32 additional female cases have been reported, suggesting that ID, MICPCH, growth retardation, axial hypotonia with or without hypertonia of extremities, and optic nerve hypoplasia are caused by loss-of-function mutations of *CASK* in female cases (Moog et al., 2011; Hayashi et al., 2012). On the other hand, a missense mutation causing a partial skipping of exon 2 of *CASK* was found in affected male individuals in an Italian family with FG syndrome, which is characterized by multiple congenital anomalies and ID (Piluso et al., 2009). More recently, five missense mutations and a splice mutation, causing amino acid changes or in-frame deletions of the CASK protein, were found in male patients and variably affected carrier female patients with ID, often accompanied by congenital nystagmus (Tarpey et al., 2009; Hackett et al., 2010). Therefore it has been postulated that hypomorphic *CASK* alleles cause ID in male individuals. Collectively, mutations of *CASK* could cause a wide spectrum of ID, ranging from nonsyndromic mild ID to syndromic severe ID with structural brain abnormalities in both male and female patients.

Herein, we report on two male patients with OS, cerebellar hypoplasia, and multiple congenital anomalies. One patient had a *CASK* deletion and the other had a mutation at the translation initiation codon, both likely leading to a loss of CASK function. Detailed clinical and molecular data are presented.

Methods

Patients

A total of 34 Japanese patients (20 male and 14 female) with OS were analyzed for copy number aberrations. Twelve of them were additionally analyzed by whole exome sequencing. The diagnosis was made based on clinical features and characteristic patterns on EEG. Mutations in *STXBP1* were not identified in these patients (including Patients 1 and 2) by high-resolution melting analysis. Thirteen male patients, including Patient 1, and three female Patients were negative for *ARX* mutation. The experimental protocols were approved by the Yokohama City University School of Medicine Institutional Review Boards for Ethical Issues. Written informed consent was obtained from all individuals and/or their families in compliance with the relevant Japanese regulations.

Genomic microarray and cloning of deletion breakpoint

Genomic DNA obtained from peripheral blood leukocytes was used. Copy number alterations were studied by using Cytogenetics Whole-Genome 2.7M Array (Affymetrix, Santa Clara, CA, U.S.A.) for 30 patients and GeneChip Human Mapping 250K NspI (Affymetrix) for four patients. Copy number alterations were analyzed using the Chromosome Analysis Suite (ChAS; Affymetrix) with NA30.1 (hg18) annotations (for 2.7M Array) or using CNAG2.0 (for 250K) (Nannya et al., 2005). The junction fragment spanning the deletion was amplified by long polymerase chain reaction (PCR), using several primer sets based on putative breakpoints from the microarray data. The junction fragment was amplified using following primers: forward, 5′-ACCCAGCGTTTCACCAAGGTCTCT-3′; reverse, 5′-GTGGCTTCAGAATTAGGCCCACAAA-3′ (product size = 1,136 bp). PCR products were electrophoresed in agarose gels, stained with ethidium bromide, extracted from the gels using a QIAquick Gel extraction kit (Qiagen, Tokyo, Japan), and sequenced.

Quantitative real-time PCR

The deletion of *CASK* was analyzed using the patient's and parental genomic DNA by quantitative real-time PCR (qPCR) on a Rotor-Gene Q thermal cycling system (Qiagen). DNA extracted from two independent blood samples each from the patient and mother were used for analysis. PCR was performed in a volume of 15 μl containing 10 ng of genomic DNA, 1× Rotor-Gene SYBR Green PCR Master Mix (Qiagen), and 1.0 μM each primer. qPCR was carried out using the two standard curve relative quantification method with four standard samples including 30, 10, 3.33, and 1.11 ng DNA, respectively. Three primer sets for exons 2, 3, and 4 of *CASK*, and one reference primer set for an area on chromosome 9 were used. Relative copy number of test regions was calculated in comparison with that of the reference region. The experiments were independently repeated three times. The data were averaged, and the standard deviation was calculated. Primer information is available on request.

Fluorescent in situ hybridization (FISH)

RP11-977L20 covering the deletion of *CASK* was labeled with SpectrumGreen -11-dUTP (Abbott, Tokyo, Japan) by nick translation. Probe-hybridization mixtures (15 μl) were denatured at 70°C for 5 min, applied to chromosomes, incubated at 37°C for 20 h, and then washed and mounted with antifade solution (Vector Laboratories, Burlingame, CA, U.S.A.) containing 4,6-diamidino-2-phenylindole. Photographs were taken on an AxioCam MR Charge Coupled Device camera fitted to an Axioplan2 fluorescence microscope (Carl Zeiss, Tokyo, Japan). The mosaic ratio was examined by two independent investigators, who each counted 100 interphase nuclei.

RNA analysis

RNA analysis using lymphoblastoid cell lines was performed as described previously (Saitsu et al., 2011). Briefly, total RNA was extracted using an RNeasy Plus Mini Kit (Qiagen); 2 μg of total RNA was subjected to reverse transcription, and 1 μl of cDNA was used for PCR.

Primer sequences are ex1-F (5′-ATGTGTACGAGCTGT GCGAGGTGAT-3′) and ex4-R (5′-AGCGTCAGCTCGCT TTACGATTTCA-3′). Two separately extracted RNA samples were used in each duplicated experiment. The DNA in each PCR band was purified using a QIAquick Gel extraction kit (Qiagen) and sequenced.

Whole exome sequencing

DNAs were captured using the SureSelect^{XT} Human All Exon 50 Mb Kit (Agilent Technologies, Santa Clara, CA, U.S.A.) and sequenced with one lane per sample on an Illumina GAIIx platform (Illumina, San Diego, CA, U.S.A.) with 108-bp paired-end reads. Image analysis and base calling were performed by sequence control software real-time analysis and CASAVA software v1.7 (Illumina). A total of 94,106,348 paired-end reads were obtained for Patient 2 and aligned to the human reference genome sequence (GRCh37/hg19) using MAQ (Li et al., 2008) and NextGENe software v2.00 with sequence condensation by consolidation (SoftGenetics, State College, PA, U.S.A.). Single nucleotide variants (SNVs) were called using MAQ and NextGENe. Small insertions and deletions were detected using NextGENe. Called SNVs were annotated with SeattleSeq Annotation. The number of variants identified by exome sequencing in Patient 2 is shown in Table S1.

Immunoblotting

Lymphoblastoid cells were washed twice in ice-cold phosphate-buffered saline (PBS), and lysed in sodium dodecyl sulfate sample buffer. Samples were size-fractionated by sodium dodecyl sulfate–polyacrylamide gel electrophoresis, transferred to the polyvinylidene fluoride membrane, and analyzed with anti-CASK monoclonal antibody, which is produced by a synthetic peptide corresponding to residues surrounding Glu327 of human CASK protein (1:1,000 dilution, D24B12; Cell Signaling, Tokyo, Japan). Anti-Lamin B polyclonal antibody (1:500 dilution, sc-6217; Santa Cruz Biotechnology Inc., Santa Cruz, CA, U.S.A.) was used as a control. Secondary antibody was peroxidase-conjugated goat anti-rabbit IgG or bovine anti-goat IgG (Jackson ImmunoResearch, West Grove, PA, U.S.A.). Blots were detected using the Supersignal West dura (Pierce, Yokohama, Japan). Chemiluminescence was visualized using a FluorChem 8900 (Alpha Innotech, San Leandro, CA, U.S.A.). Experiments were repeated twice using two separately prepared samples.

Results

Clinical information

Patient 1 is a 4-year-old boy born to nonconsanguineous parents. The pregnancy was uneventful, and he was born at term (gestational age 41 weeks and 2 days) with induced labor but no asphyxia. His body weight was 2,606 g (−2.0 standard deviation [SD]), his height was 47.5 cm (−1.4 SD), and his head circumference was 32.2 cm (−1.2 SD). An apneic event with cyanosis, which was not improved by positioning or oxygen inhalation, was evident 2 days after birth. Brain magnetic resonance imaging (MRI) demonstrated prominent cerebellar hypoplasia (Fig. 1A). EEG showed multifocal epileptic discharges with a short period (1 s) of flat basic rhythm (Fig. 1C, left). Phenobarbital was administered at 21 days and was effective for the apneic event. At the age of 2 months, he developed daily clustering of tonic seizures with suppression-burst pattern on both awake and asleep EEG (Fig. 1C, right)and poor feeding. EEG at 5 months demonstrated hypsarrhythmia, which is characteristically seen in West syndrome. He exhibited long slender fingers, micropenis, micrognathia, and a short neck with obstructive respiration, and then required tracheostomy with laryngotracheal separation and gastrostomy. His head circumference was 47.1 cm (−2.7 SD) at 1 years and 4 months. On examination at 4 years, he was bedridden and unable to track objects. Tonic seizures lasting 10–30 s several times a day and frequent myoclonic seizures were seen regardless of treatment with phenobarbital, pyridoxal phosphate, zonisamide, clobazam, and lamotrigine. EEG during sleep at 3 years of age demonstrated multifocal sharp and slow-wave complexes and diffuse low-voltage fast-wave bursts or a desynchronization pattern.

Patient 2 is a 4-year-old boy born to nonconsanguineous parents. He was born at 39 weeks of gestation without asphyxia after uneventful pregnancy. His body weight was 2,000 g (−3.3 SD), his height was 43.0 cm (−2.8 SD), and his head circumference was 29.5 cm (−2.7 SD). He was poorly fed with milk and referred to us at 27 days after birth. Multiple anomalies were recognized such as micrognathia, high arched palate, shortened upper arms, bilateral overlapping fingers and clinodactyly, and persistent hypertrophic primary vitreous. He underwent ophthalmic surgery at 33 days after birth. Brain MRI demonstrated prominent cerebellar hypoplasia (Fig. 1B). At 3 months of age, he showed frequent generalized tonic seizures, and EEG showed a suppression-burst pattern in both awake and asleep states (Fig. 1D). He showed normal auditory brain responses. Laboratory data, including lactate, pyruvate, and very long fatty acids, were all normal. Phenobarbital was initiated and only partially effective for his seizures. Topiramate, clobazam, and sodium bromide were added, and seizure frequencies were decreased from daily to weekly. His development was severely delayed with no head control or eye pursuit. His deep tendon reflexes are exaggerated, with positive bilateral Babinski signs. He shows muscle hypertonus with rigidity of both upper and lower limbs.

Copy number analysis

Through screening for copy number alterations by genomic microarray analysis, we identified an approximately 110-kb microdeletion involving exon 2 of *CASK* at Xp11.4 in Patient 1 (Fig. 2A). Breakpoint-specific PCR analysis of

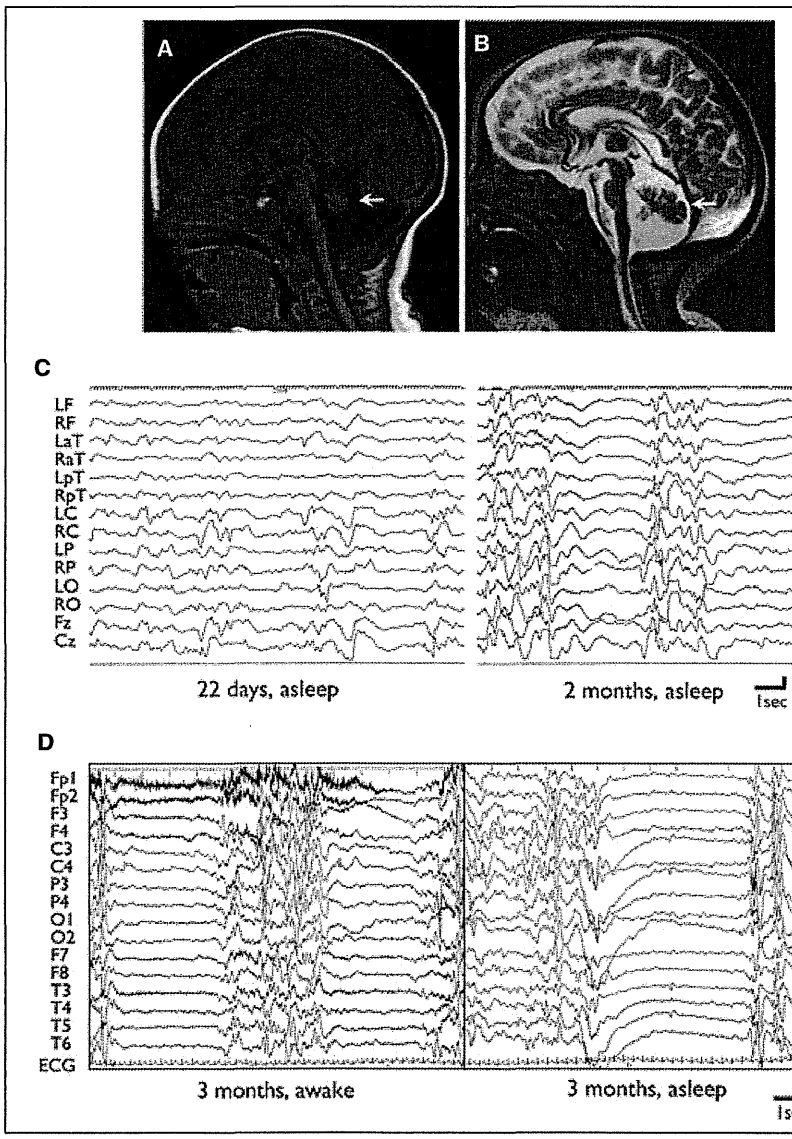

Figure 1.
Brain MRI findings in the patients. (**A**) T_1-weighted midline sagittal image of Patient 1 at age 21 days. (**B**) T_2-weighted midline sagittal image of Patient 2 at age 3 months. Both patients showed prominent cerebellar hypoplasia (arrows). (**C**) EEG of Patient 1 showed multifocal sharp wave or irregular sharp-and-slow wave complex but no diffuse epileptic discharges at age 22 days (left) and diffuse high-amplitude slow-wave burst mixed with irregular spike or sharp wave interrupted by low-amplitude activity (suppression-burst) at age 2 months (right). (**D**) EEG of Patient 2 at age 3 months. High-voltage bursts alternate with almost flat suppression phases at an approximately regular rate in both awake and asleep states.
Epilepsia © ILAE

the family showed that the deletion was inherited from his mother (Fig. 2B). The sequence of the junctional fragment confirmed a 111,172-bp deletion (NG_016754.1: g.17883_129055del) (Fig. 2C). Sequencing also identified 5-bp duplicated sequences as well as a 2-bp insertion at the deletion junction. We were surprised that the healthy mother possessed this deletion, because the deletion is predicted to lead to a frameshift with presumably premature termination of the translation. The deletion was further examined by qPCR and FISH analyses. Whereas the relative copy numbers of exons 3 and 4 (not deleted) were nearly 1.0 in the two maternal DNA samples, as expected, those for deleted exon 2 in the two samples were 0.67 and 0.81 (Fig. 2D). Because the relative copy number is expected to be 0.5 if one of two copies is deleted (as the healthy father showed), this result suggested that the mother may be somatic mosaic for the deletion. In fact, FISH analysis revealed that only 40 of 200 interphase nuclei showed one clear signal and another weaker signal, consistent with partial deletion within the bacterial artificial chromosome probe (Fig. 2E). Based on these findings, we concluded that the mother is somatic mosaic for the deletion, and that the percentage of mosaicism is approximately 20%. To explore the effect of the deletion on the transcription of *CASK*, reverse transcriptase PCR designed to amplify exons 1–4 was performed using total RNA extracted from lymphoblastoid cell lines (LCLs) derived from the patient and his mother (Fig. 2F). A single band (299-bp) corresponding to the wild-type *CASK* allele was amplified using a complementary DNA (cDNA) template from a control LCL (Fig. 2F). By contrast, only a smaller band, in which exon 2 had been deleted, was detected from the patient's cDNA

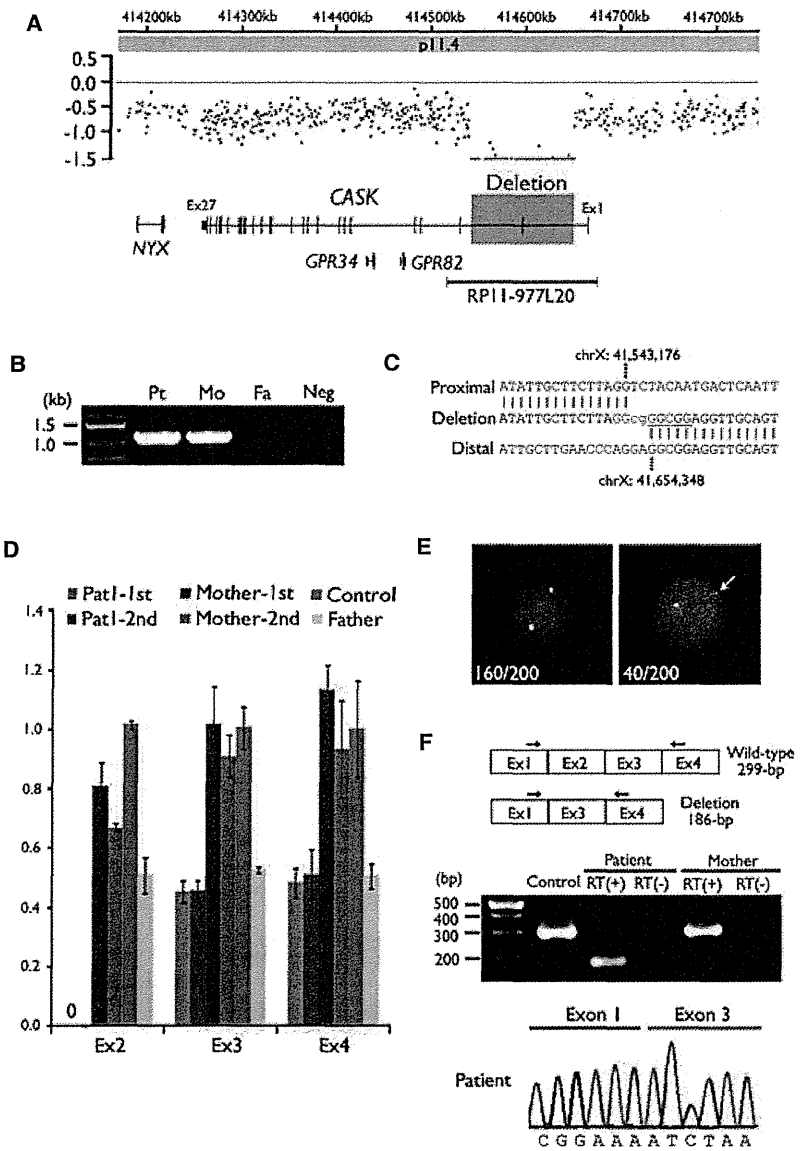

Figure 2.

A 111-kb deletion involving exon 2 of *CASK*. (**A**) The 2.7M array profile clearly shows a deletion involving exon 2 of *CASK* at Xp11.4. The x- and y-axes show the genomic location from the p telomere of chromosome X (UCSC coordinates, May, 2006) and $\log_2$ signal ratio values, respectively. Four RefSeq genes including *CASK* and RP11-977L20 clone used for FISH are shown. (**B**) Breakpoint-specific PCR analysis of the family. Primers flanking the deletion were able to amplify a 1,136-bp product from both the Patient 1 and his mother. Pt, patient; Mo, mother; Fa, Father; Neg, negative control (no template DNA). (**C**) Deletion junction sequence. Top, middle, and bottom strands show proximal, deleted and distal sequences, respectively. The two nucleotides inserted are presented in lower case. A 5-bp sequence that appears twice at the breakpoint region is colored red or underlined. (**D**) qPCR analysis of the family, and a female control. Two DNA samples extracted from two independent blood samples were used for analysis of the patient and his mother. Relative copy numbers of deleted exon 2 were 0.67 and 0.81 (both above 0.5) in the mother, suggesting somatic mosaicism of the deletion. (**E**) FISH images of RP11-977L20, covering the deletion, on the mother's chromosomes. One-hundred sixty nuclei showed two clear signals (left), and 40 nuclei showed one clear signal and a weaker signal (right, white arrow) consistent with partial deletion within the probe. (**F**) Schematic representation of the transcript from exons 1–4 of *CASK*. Exons and primers are depicted as boxes and arrows, respectively (top). A single wild-type amplicon was detected in a control and the mother. A smaller product was amplified only from the patient's cDNA. RT (+): with reverse transcriptase, RT (–): without reverse transcriptase as a negative control. Sequence of a smaller amplicon clearly demonstrated the exon 2 deletion (bottom).

(Fig. 2F). The smaller mutant band was not detected from the mother's cDNA (Fig. 2F). Human androgen receptor assay showed that X-inactivation was random (70:30) in the mother (data not shown). However, because the percentage of mosaicism was low (20%), it remains possible that the deletion allele may undergo X-inactivation in cells possessing it, leading to diminished expression of the deletion allele in LCL.

Whole exome sequencing

To find potential pathologic mutations, whole exome sequencing of 12 patients was performed. We focused on mutations in *CASK*, and identified a hemizygous c.1A>G mutation of the first ATG codon in Patient 2 (Fig. 3A,B). This mutation is anticipated to result in alternative ATG codon usage. By using the next downstream in-frame ATG codon positioned at c.202_204 (Fig. 3C), a truncated protein without the first 67 amino acids containing calmodulin-dependent kinase domain could be produced, although this ATG codon (CATATGC) does not conform to the Kozak consensus. The parental DNA did not have the mutation, suggesting that the mutation occurred de novo (Fig. 3B). No *CASK* mutations were found in any of the other patients.

Immunoblotting

To evaluate mutational effect for CASK expression in two patients, immunoblotting was performed using total lysate of LCL. A strong signal at 104 kDa was detected in a control and the mother of Patient 1, showing strong expression of wild-type CASK protein in LCLs (Fig. 4, top). However, both Patients 1 and 2 did not show any detectable signal (Fig. 4, top), whereas the Lamin B showed comparable expression in all samples loaded (Fig. 4, bottom). Thus these data suggest that expression of CASK protein was severely decreased in two patients.

Discussion

We describe two male patients possessing an intragenic *CASK* deletion (only exon 2) or a hemizygous c.1A>G

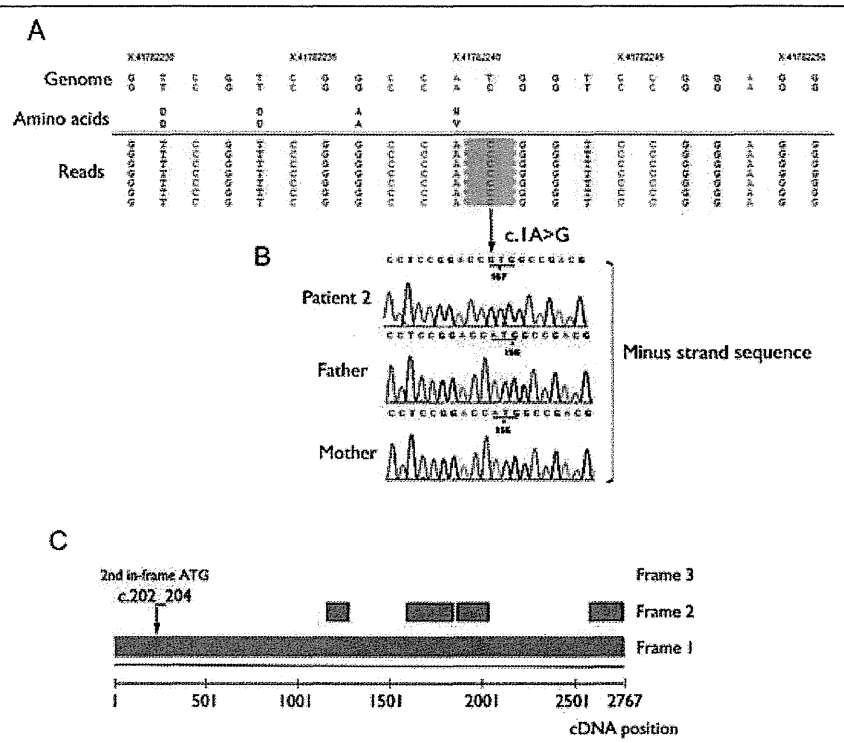

Figure 3.
c.1A>G mutation identified by exome sequencing. (**A**) From top to bottom, genomic sequence (plus strand), coding amino acids, and sequence reads covering the site of the pathogenic mutation. In genomic sequence and amino acids, upper and lower indicate reference and mutant alleles, respectively. There are six reads showing a hemizygous T>C transition at position 41,782,240 of chromosome X. (**B**) Validation of the c.1A>G mutation and inheritance analysis by Sanger sequencing. The mutation position is indicated by the arrow. (**C**) Possible open reading frames within the coding region of the *CASK* transcript (NM_003688.3). Open reading frames longer than 100 bp are shown in blue squares. The second in-frame ATG codon is positioned at c.202_204 (arrow). Any proteins longer than the protein utilizing the second in-frame ATG codon are not predicted.

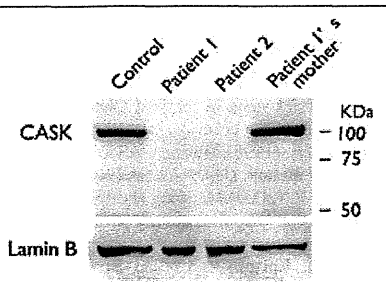

Figure 4.
Expression of CASK protein in LCL. Immunoblot analysis by using a monoclonal CASK antibody (top). Expression of CASK protein was not detected in LCL derived from two patients, whereas LCL of a control and Patient 1's mother showed strong CASK expression. The observed differences in expression were not due to difference of loading conditions, because the level of Lamin B protein was similar in all cases (bottom).

mutation. In Patient 1, the deletion is likely to be an almost null mutation as the mutant *CASK* transcript with exon 2 deletion has a frameshift with premature termination. Deletions in *CASK* have been reported in 16 female patients, and a skewed X-inactivation pattern was observed in two of them (the others had random inactivation pattern or not determined) (Froyen et al., 2007; Hayashi et al., 2008; Najm et al., 2008; Moog et al., 2011; Hayashi et al., 2012). Of interest, partial skipping of the exon 2 of *CASK* (approximately 3–6% of the unskipped transcripts) has been reported in male patients with FG syndrome showing ID, relative macrocephaly, hypotonia, severe constipation, and behavioral disturbance (Piluso et al., 2003, 2009). By contrast, our Patient 1 with complete deletion of exon 2 showed a more severe phenotype, suggesting that he showed one of the most severe phenotypes caused by *CASK* abnormalities. In Patient 2, the mutation of the first ATG codon could produce a truncated protein without the amino terminal 67 amino acids. However, this alternative in-frame ATG codon does not conform to the Kozak consensus, suggesting that its translation would be significantly reduced. In fact, CASK protein was not detected in the LCL of two patients, suggesting that expression of CASK protein should be extremely low. Because only partial skipping of exon 9 (about 20% of the mutant transcripts) (Najm et al., 2008) or of exon 2 (3–6% of the unskipped transcripts) (Piluso et al., 2009) is sufficient to cause ID and other features in male cases, it is likely that the maintenance of expression level of functional CASK protein is essential.

Two male patients with *CASK* abnormalities showed typical OS features, revealing an association between OS and *CASK* abnormalities in male patients, which has to date never been shown. Microcephaly and prominent cerebellar hypoplasia were also recognized, consistent with previous reports (Najm et al., 2008; Moog et al., 2011; Hayashi et al., 2012). Of interest, our patients also showed reduced body size and multiple congenital anomalies such as high arched palate, micrognathia, finger anomalies, and persistent hypertrophic primary vitreous. This suggests that *CASK* may be involved in overall body growth and development of these organs in humans. Supporting this idea, growth retardation and small jaw have been reported in patients with *CASK* abnormalities (Najm et al., 2008; Hackett et al., 2010; Moog et al., 2011). In addition, *CASK*-deficient mice showed micrognathia and cleft palate with male lethality (Laverty & Wilson, 1998), and hypomorphic *CASK* mutant mice are significantly smaller than littermate control mice (Atasoy et al., 2007). Therefore, it is likely that loss-of-function mutations in *CASK* cause reduced body size and multiple congenital anomalies, as well as OS and cerebellar hypoplasia.

The same deletion was found in both the mother and the affected son, indicating a germline mosaicism in the mother associated with recurrence risks. This information is useful for genetic counseling in the family. The maternal somatic mosaicism was confirmed by different methods including FISH, qPCR, and breakpoint-specific PCR analyses. We would like to emphasize the importance of breakpoint-specific PCR analysis, in which a specific band undoubtedly indicates the presence of the deletion allele. Because PCR is a powerful tool for amplifying target sequences, we could easily detect the somatic mosaic, even though it existed in approximately 20% of cells. In addition, it has been reported that PCR analyses of the deletion junction can detect extremely low-level mosaicism not detected by array comparative genomic hybridization (Zhang et al., 2009). The increasing density of available oligonucleotide arrays allows us to design long (or even regular) PCR primers for junctional cloning. Once junctional cloning is successful (though it is sometimes difficult), it is highly useful for examining parental states.

It has been determined that mutations in three genes (*STXBP1*, *ARX*, and *CASK*) cause OS. Screening for *STXBP1* mutations should be considered in OS patients with no brain anomalies in both male and female patients. Screening for *ARX* mutations would be reasonable in male patients with OS, and the presence of micropenis may encourage its screening (Kato et al., 2007). Based on this study, *CASK* mutations should be considered in patients with OS and cerebellar hypoplasia.

In conclusion, we report for the first time *CASK* abnormalities in male individuals with OS. Maternal somatic mosaicism of a *CASK* deletion is also described, suggesting that somatic and germline mosaicism of a microdeletion should be carefully considered in the examination of parental samples. Our data expand the clinical spectrum of *CASK* mutations to include OS with cerebellar hypoplasia and congenital anomalies at the most severe end of clinical presentation.

Acknowledgments

We would like to thank the patients and their families for their participation in this study. This work was supported by Research Grants from the Ministry of Health, Labour and Welfare (H.S., M.K., H.O. N. Miyake, and N. Matsumoto), a Grant-in-Aid for Scientific Research from Japan Society for the Promotion of Science (M.K., H.O., N. Miyake, and N. Matsumoto), a Grant-in-Aid for Young Scientist from Japan Society for the Promotion of Science (H.S., H.D., and N. Miyake), a grant from the Japan Science and Technology Agency (N. Matsumoto), the Strategic Research Program for Brain Sciences (N. Matsumoto), and a Grant-in-Aid for Scientific Research on Innovative Areas (Foundation of Synapse and Neurocircuit Pathology) from the Ministry of Education, Culture, Sports, Science and Technology of Japan (N. Matsumoto), Research Grants from the Japan Epilepsy Research Foundation (H.S. and M.K.), a Research Grant from Naito Foundation (N. Matsumoto), and Research Grants from Takeda Science Foundation (N. Miyake and N. Matsumoto). This work was performed at the Advanced Medical Research Center, Yokohama City University, Japan.

Disclosure

None of the authors has any conflict of interest to disclose. We confirm that we have read the Journal's position on issues involved in ethical publication and affirm that this report is consistent with those guidelines.

References

Atasoy D, Schoch S, Ho A, Nadasy KA, Liu X, Zhang W, Mukherjee K, Nosyreva ED, Fernandez-Chacon R, Missler M, Kavalali ET, Sudhof TC. (2007) Deletion of CASK in mice is lethal and impairs synaptic function. *Proc Natl Acad Sci U S A* 104:2525–2530.

Djukic A, Lado FA, Shinnar S, Moshe SL. (2006) Are early myoclonic encephalopathy (EME) and the Ohtahara syndrome (EIEE) independent of each other? *Epilepsy Res* 70(Suppl. 1):S68–S76.

Froyen G, Van Esch H, Bauters M, Hollanders K, Frints SG, Vermeesch JR, Devriendt K, Fryns JP, Marynen P. (2007) Detection of genomic copy number changes in patients with idiopathic mental retardation by high-resolution X-array-CGH: important role for increased gene dosage of XLMR genes. *Hum Mutat* 28:1034–1042.

Fullston T, Brueton L, Willis T, Philip S, MacPherson L, Finnis M, Gecz J, Morton J. (2010) Ohtahara syndrome in a family with an ARX protein truncation mutation (c.81C>G/p.Y27X). *Eur J Hum Genet* 18:157–162.

Giordano L, Sartori S, Russo S, Accorsi P, Galli J, Tiberti A, Bettella E, Marchi M, Vignoli A, Darra F, Murgia A, Bernardina BD. (2010) Familial Ohtahara syndrome due to a novel *ARX* gene mutation. *Am J Med Genet A* 152A:3133–3137.

Hackett A, Tarpey PS, Licata A, Cox J, Whibley A, Boyle J, Rogers C, Grigg J, Partington M, Stevenson RE, Tolmie J, Yates JR, Turner G, Wilson M, Futreal AP, Corbett M, Shaw M, Gecz J, Raymond FL, Stratton MR, Schwartz CE, Abidi FE. (2010) *CASK* mutations are frequent in males and cause X-linked nystagmus and variable XLMR phenotypes. *Eur J Hum Genet* 18:544–552.

Hayashi S, Mizuno S, Migita O, Okuyama T, Makita Y, Hata A, Imoto I, Inazawa J. (2008) The *CASK* gene harbored in a deletion detected by array-CGH as a potential candidate for a gene causative of X-linked dominant mental retardation. *Am J Med Genet A* 146A:2145–2151.

Hayashi S, Okamoto N, Chinen Y, Takanashi JI, Makita Y, Hata A, Imoto I, Inazawa J. (2012) Novel intragenic duplications and mutations of CASK in patients with mental retardation and microcephaly with pontine and cerebellar hypoplasia (MICPCH). *Hum Genet* 131:99–110.

Hsueh YP. (2006) The role of the MAGUK protein CASK in neural development and synaptic function. *Curr Med Chem* 13:1915–1927.

Kato M, Saitoh S, Kamei A, Shiraishi H, Ueda Y, Akasaka M, Tohyama J, Akasaka N, Hayasaka K. (2007) A longer polyalanine expansion mutation in the *ARX* gene causes early infantile epileptic encephalopathy with suppression-burst pattern (Ohtahara Syndrome). *Am J Hum Genet* 81:361–366.

Kato M, Koyama N, Ohta M, Miura K, Hayasaka K. (2009) Frameshift mutations of the *ARX* gene in familial Ohtahara syndrome. *Epilepsia* 51:1679–1684.

Laverty HG, Wilson JB. (1998) Murine CASK is disrupted in a sex-linked cleft palate mouse mutant. *Genomics* 53:29–41.

Li H, Ruan J, Durbin R. (2008) Mapping short DNA sequencing reads and calling variants using mapping quality scores. *Genome Res* 18:1851–1858.

Moog U, Kutsche K, Kortum F, Chilian B, Bierhals T, Apeshiotis N, Balg S, Chassaing N, Coubes C, Das S, Engels H, Van Esch H, Grasshoff U, Heise M, Isidor B, Jarvis J, Koehler U, Martin T, Oehl-Jaschkowitz B, Ortibus E, Pilz DT, Prabhakar P, Rappold G, Rau I, Rettenberger G, Schluter G, Scott RH, Shoukier M, Wohlleber E, Zirn B, Dobyns WB, Uyanik G. (2011) Phenotypic spectrum associated with CASK loss-of-function mutations. *J Med Genet* 48:741–751.

Najm J, Horn D, Wimplinger I, Golden JA, Chizhikov VV, Sudi J, Christian SL, Ullmann R, Kuechler A, Haas CA, Flubacher A, Charnas LR, Uyanik G, Frank U, Klopocki E, Dobyns WB, Kutsche K. (2008) Mutations of CASK cause an X-linked brain malformation phenotype with microcephaly and hypoplasia of the brainstem and cerebellum. *Nat Genet* 40:1065–1067.

Nannya Y, Sanada M, Nakazaki K, Hosoya N, Wang L, Hangaishi A, Kurokawa M, Chiba S, Bailey DK, Kennedy GC, Ogawa S. (2005) A robust algorithm for copy number detection using high-density oligonucleotide single nucleotide polymorphism genotyping arrays. *Cancer Res* 65:6071–6079.

Ohtahara S, Yamatogi Y. (2006) Ohtahara syndrome: with special reference to its developmental aspects for differentiating from early myoclonic encephalopathy. *Epilepsy Res* 70(Suppl. 1):S58–S67.

Ohtahara S, Ishida T, Oka E, Yamatogi Y, Inoue H, Karita S, Ohtsuka Y. (1976) [On the specific age dependent epileptic syndrome: the early-infantile epileptic encephalopathy with suppression-burst.]. *No to Hattatsu* 8:270–279.

Piluso G, Carella M, D'Avanzo M, Santinelli R, Carrano EM, D'Avanzo A, D'Adamo AP, Gasparini P, Nigro V. (2003) Genetic heterogeneity of FG syndrome: a fourth locus (FGS4) maps to Xp11.4-p11.3 in an Italian family. *Hum Genet* 112:124–130.

Piluso G, D'Amico F, Saccone V, Bismuto E, Rotundo IL, Di Domenico M, Aurino S, Schwartz CE, Neri G, Nigro V. (2009) A missense mutation in *CASK* causes FG syndrome in an Italian family. *Am J Hum Genet* 84:162–177.

Saitsu H, Kato M, Mizuguchi T, Hamada K, Osaka H, Tohyama J, Uruno K, Kumada S, Nishiyama K, Nishimura A, Okada I, Yoshimura Y, Hirai S, Kumada T, Hayasaka K, Fukuda A, Ogata K, Matsumoto N. (2008) De novo mutations in the gene encoding STXBP1 (MUNC18-1) cause early infantile epileptic encephalopathy. *Nat Genet* 40:782–788.

Saitsu H, Kato M, Okada I, Orii KE, Higuchi T, Hoshino H, Kubota M, Arai H, Tagawa T, Kimura S, Sudo A, Miyama S, Takami Y, Watanabe T, Nishimura A, Nishiyama K, Miyake N, Wada T, Osaka H, Kondo N, Hayasaka K, Matsumoto N. (2010) *STXBP1* mutations in early infantile epileptic encephalopathy with suppression-burst pattern. *Epilepsia* 51:2397–2405.

Saitsu H, Hoshino H, Kato M, Nishiyama K, Okada I, Yoneda Y, Tsurusaki Y, Doi H, Miyake N, Kubota M, Hayasaka K, Matsumoto N. (2011) Paternal mosaicism of an *STXBP1* mutation in OS. *Clin Genet* 80:484–488.

Tarpey PS, Smith R, Pleasance E, Whibley A, Edkins S, Hardy C, O'Meara S, Latimer C, Dicks E, Menzies A, Stephens P, Blow M, Greenman C, Xue Y, Tyler-Smith C, Thompson D, Gray K, Andrews J, Barthorpe S, Buck G, Cole J, Dunmore R, Jones D, Maddison M, Mironenko T, Turner R, Turrell K, Varian J, West S, Widaa S, Wray P, Teague J, Butler A, Jenkinson A, Jia M, Richardson D, Shepherd R, Wooster R, Tejada MI, Martinez F, Carvill G, Goliath R, de Brouwer APM, van Bokhoven H, Van Esch H, Chelly J, Raynaud M, Ropers H-H, Abidi FE, Srivastava AK, Cox J, Luo Y, Mallya U, Moon J, Parnau J, Mohammed S, Tolmie JL, Shoubridge C, Corbett M, Gardner A, Haan E, Rujirabanjerd S, Shaw M, Vandeleur L, Fullston T, Easton DF, Boyle J, Partington M, Hackett A, Field M, Skinner C, Stevenson RE,

Bobrow M, Turner G, Schwartz CE, Gecz J, Raymond FL, Futreal PA, Stratton MR. (2009) A systematic, large-scale resequencing screen of X-chromosome coding exons in mental retardation. *Nat Genet* 41:535–543.

Yamatogi Y, Ohtahara S. (2002) Early-infantile epileptic encephalopathy with suppression-bursts, Ohtahara syndrome; its overview referring to our 16 cases. *Brain Dev* 24:13–23.

Zhang F, Khajavi M, Connolly AM, Towne CF, Batish SD, Lupski JR. (2009) The DNA replication FoSTeS/MMBIR mechanism can generate genomic, genic and exonic complex rearrangements in humans. *Nat Genet* 41:849–853.

Supporting Information

Additional Supporting Information may be found in the online version of this article:

Table S1. All variants identified by exome sequencing in Patient 2.

Please note: Wiley-Blackwell is not responsible for the content or functionality of any supporting information supplied by the authors. Any queries (other than missing material) should be directed to the corresponding author for the article.

Reply

Aron S. Buchman, MD,[1,2] Joshua M. Shulman, MD, PhD,[3,4] Sue E. Leurgans, PhD,[1,2] Julie A. Schneider, MD, MS,[1,2,5] and David A. Bennett, MD[1,2]

We thank Drs Jellinger and Attems for their interest in our study. In agreement with prior reports, we found that Parkinson disease (PD) pathology, including nigral neuronal loss and Lewy body pathology, is common in older adults without PD. Furthermore, we provide evidence that PD nigral pathology is related to parkinsonian motor signs in persons without a clinical diagnosis of PD.[1] This contrasts with prior studies of incidental Lewy body disease, which found associations with subtle electrophysiologic changes but not with overt motor signs.[2] Interestingly, in the current study, we also found that Alzheimer disease (AD) and cerebrovascular pathology showed independent associations with the severity of parkinsonian motor signs.[1] As requested, the correlations among these common brain pathologies are included in the accompanying Table. It is interesting that Dr Attems and colleagues did not find an association of nigral pathology or cerebrovascular disease with parkinsonian signs among persons with AD.[3] We and others have reported such associations.[4–6] Overall, the findings in the current study have important public health implications. They suggest that mild parkinsonian signs, reported in up to 50% of older adults by age 85 years and associated with significant morbidity and mortality, may be caused by a range of pathologies including PD pathology, AD, and cerebrovascular pathologies. These data underscore the need for more sensitive clinical measures and biomarkers that can detect and differentiate the various neuropathologies underlying the development of parkinsonian signs in old age.

Potential Conflicts of Interest

Nothing to report.

[1]Rush Alzheimer's Disease Center and [2]Department of Neurological Sciences, Rush University Medical Center, Chicago, IL, [3]Department of Neurology, Brigham and Women's Hospital, Boston, MA, [4]Department of Neurology, Harvard Medical School, Boston, MA, and [5]Department of Pathology (Neuropathology), Rush University Medical Center, Chicago, IL

References

1. Buchman AS, Shulman JM, Nag S, et al. Nigral pathology and parkinsonian signs in elders without Parkinson disease. Ann Neurol 2012;71:258–266.
2. Caviness JN. Presymptomatic Parkinson's disease: the Arizona experience. Parkinsonism Relat Disord 2012;18(suppl 1):S203–S206.
3. Attems J, Quass M, Jellinger K. Tau and α-synuclein brainstem pathology in Alzheimer disease: relation with extrapyramidal signs. Acta Neuropathol 2007;113:53–62.
4. Burns JM, Galvin JE, Roe CM, et al. The pathology of the substantia nigra in Alzheimer disease with extrapyramidal signs. Neurology 2005;64:1397–1403.
5. Schneider JA, Li JL, Li Y, et al. Substantia nigra tangles are related to gait impairment in older persons. Ann Neurol 2006;59:166–173.
6. Buchman AS, Leurgans SE, Nag S, et al. Cerebrovascular disease pathology and parkinsonian signs in old age. Stroke 2011;42:3183–3189.

DOI: 10.1002/ana.23639

Whole Exome Sequencing Identifies *KCNQ2* Mutations in Ohtahara Syndrome

Hirotomo Saitsu, MD, PhD,[1] Mitsuhiro Kato, MD, PhD,[2] Ayaka Koide, MD, PhD,[3] Tomohide Goto, MD, PhD,[3] Takako Fujita, MD,[4] Kiyomi Nishiyama, PhD,[1] Yoshinori Tsurusaki, PhD,[1] Hiroshi Doi, MD, PhD,[1] Noriko Miyake, MD, PhD,[1] Kiyoshi Hayasaka, MD, PhD,[2] and Naomichi Matsumoto, MD, PhD[1]

Recently, Weckhuysen et al revealed that *KCNQ2* mutations are involved in a substantial proportion of patients with a neonatal epileptic encephalopathy.[1] Some cases showed a suppression–burst pattern on electroencephalogram (EEG), tonic seizures, and profound intellectual disability, resembling Ohtahara syndrome (OS). By whole exome sequencing analysis of 12

TABLE: Intercorrelation of Postmortem Indices

Index	Macroinfarcts	Microinfarcts	Arteriolosclerosis	AD Pathology	Nigral Lewy Bodies
Nigral neuronal loss	0.07, 0.068	0.02, 0.628	0.13, <0.001	0.14, <0.001	0.38, <0.001
Macroinfarcts	—	0.39, 0.056	0.26, <0.001	0.09, 0.017	−0.063, 0.072
Microinfarcts		—	0.15, <0.001	0.04, 0.315	−0.10, 0.075
Arteriolosclerosis			—	0.03, 0.385	0.03, 0.491
AD pathology				—	0.07, 0.052

Based on Spearman or tetrachoric correlation and *p* value.

TABLE: Summary of the Clinical Features of Subjects with *KCNQ2* Mutations

Case #	Mutation	Sex	Age	Age at Onset, Days	Initial Symptoms	Initial Epileptic Attacks	Initial EEG	Age at Onset of Spasms, Days	Age at Onset of SB Pattern, Days	Response to Therapy	Other Drugs Used, but Ineffective	Development	Neurological Examination	Involuntary Movement
1469	c.1010C>G (p.A337G) de novo	M	7 years	7	Vomiting	7 days, tonic seizure	SB	—	22	Seizure free and SB on EEG, disappeared after high-dose PB, CPS since age 5 years	B6, ZNS	No meaningful words, able to crawl, stand with support	Severe MR, no pyramidal signs	No
1654	c.341C>T (p.T114I) de novo	F	7 years	0	Tremor of the upper extremities	2 days, generalized convulsion with cyanosis	SB	—	2	Seizure free after ZNS, CPS since age 5 years	B6, CZP, PHT	DQ 10, bed-ridden, smiling	Profound MR, spastic quadriplegia	No
1754	c.794C>T (p.A265V) de novo	M	3 months	1	Apneic spell	1 days, tonic spasms with right opsoclonuslike movement	SB	1	2	Intractable	B6, ZNS, VPA, CZP, CBZ	Delayed, no eye pursuit	Unknown	Myoclonus at the bilateral upper extremities

B6 = vitamin B6; CBZ = carbamazepine; CPS = complex partial seizures; CZP = clonazepam; DQ = developmental quotient; EEG = electroencephalogram; MR = mental retardation; PB = phenobarbital; PHT = phenytoin; SB = suppression–burst; VPA = valproic acid; ZNS = zonisamide.

patients with OS, we found 3 missense mutations in *KCNQ2* (25%): c.341C>T (p.T114I), c.1010C>G (p.A337G), and c.794C>T (p.A265V) in 3 patients. All 3 patients showed initial seizures early in the neonatal period and a characteristic suppression–burst pattern on EEG, leading to diagnosis as OS (Table). Seizures were temporarily well controlled in 2 patients. Consistent with Weckhuysen's report, in which 6 of 8 mutations arose de novo, the 3 mutations in our series are de novo changes. Thus, it is likely that de novo *KCNQ2* mutations are among the common causes of early onset epileptic encephalopathies, including OS. *KCNQ2* mutations have been shown to cause benign familial neonatal seizures, which is distinct from OS.[2,3] We unexpectedly found *KCNQ2* mutations by whole exome sequencing. Exome sequencing using familial trios (patients and their parents) can identify de novo mutations.[4] Novel associations between unexpected gene mutations and early onset epileptic encephalopathies may be validated by such new technologies.

Acknowledgment

Supported by a research grant from the Ministry of Health, Labor, and Welfare, Japan (H.S., M.K., N.Mi., N.Ma.), a Grant-in-Aid for Scientific Research from the Japan Society for the Promotion of Science (H.S., M.K., N.Mi., N.Ma.), a research grant from the Japan Science and Technology Agency (N.Ma.), and the Strategic Research Program for Brain Sciences (a Grant-in-Aid for Scientific Research on Innovative Areas, Foundation of Synapse and Neurocircuit Pathology; N.Ma.).

Potential Conflicts of Interest

Nothing to report.

[1]Department of Human Genetics, Yokohama City University Graduate School of Medicine, Yokohama, [2]Department of Pediatrics, Yamagata University Faculty of Medicine, Yamagata, [3]Department of Neurology, Tokyo Metropolitan Children's Medical Center, Fuchu, and [4]Department of Pediatrics, Fukuoka University Faculty of Medicine, Fukuoka, Japan

References

1. Weckhuysen S, Mandelstam S, Suls A, et al. KCNQ2 encephalopathy: emerging phenotype of a neonatal epileptic encephalopathy. Ann Neurol 2012;71:15–25.
2. Singh NA, Charlier C, Stauffer D, et al. A novel potassium channel gene, KCNQ2, is mutated in an inherited epilepsy of newborns. Nat Genet 1998;18:25–29.

3. Biervert C, Schroeder BC, Kubisch C, et al. A potassium channel mutation in neonatal human epilepsy. Science 1998;279: 403–406.
4. Vissers LE, de Ligt J, Gilissen C, et al. A de novo paradigm for mental retardation. Nat Genet 2010;42:1109–1112.

DOI: 10.1002/ana.23620

Brain Death in Children: Why Does It Have to Be So Complicated?

Thomas Nakagawa, MD,[1] Stephen Ashwal, MD,[2] Mudit Mathur, MD,[3] and Mohan Mysore, MD[4]

The authors appreciate the editorial comments by Wijdicks and Smith[1] and would like to address concerns about why the diagnosis of brain death in pediatric patients has to be "so complicated."

This revised clinical guideline focused specifically on determining brain death and deliberately excluded issues related to ethical concerns and organ donation. Failure to mention the Child Neurology Society (CNS) as the third sponsoring society of this guideline is a major oversight of the editorial.[1] CNS provided significant review by Practice Committee members and the society's Executive Board.[2] The quality of evidence provided in this guideline was equivalent to, if not more comprehensive than, the revised American Academy of Neurology (AAN) guideline, which reported only class III or IV evidence for 4 of 5 questions posed.[3] We used the GRADE system to develop a consensus guideline because no class I or II studies to determine pediatric brain death exist.[2] Interestingly, the AAN is currently revising guideline development for practicing neurologists to use a modification of the GRADE system.

A wide range of clinical entities can result in brain death in newborns, children, and adolescents. The guideline, the checklist, and Table 3 clearly state that all reversible conditions should be excluded prior to the first brain death examination. However, some uncertainty in the newborn period still exists leading to age-based observation periods. These consensus based recommendations reflect extensive clinical experience across several pediatric disciplines. Additionally, provisions for pediatric trauma patients and neonates were included. Virtually every committee member has cared for acutely injured children who met examination criteria for brain death within the initial 24 hours. Some recovered brain function although most did not which is why 2 examinations over defined time periods is recommended. The recommended time periods are consensus based rather than arbitrary time periods. Neurologic examination findings remaining unchanged and consistent with brain death throughout the observation period was one of the recommended criteria for determining brain death in the 1987 guidelines. The committee retained this recommendation in the current update. We agree that apparent neurologic improvements reported in anecdotal cases are due to diagnostic errors when critically examined; this is precisely the reason why a change in findings between examinations implies the neurological process is potentially reversible, precluding the diagnosis of brain death.

The revised guideline repeatedly states that brain death is a clinical diagnosis, and factors influencing the neurologic examination must be corrected before initiating brain death evaluation and apnea testing. Ancillary studies do not trump the neurological examination, and we clearly state that ancillary studies should not be viewed as a substitute for the neurologic examination. However, situations exist where ancillary studies are helpful to determine death. The revised guideline and checklist have simplified and clarified many previous sources of confusion. Additionally, the checklist will help standardize determination and documentation of brain death in children.[4]

Prolonging declaration of death does not appear to be a major concern in children—perhaps differing from the experience in adults. Families appreciate the added certainty conferred by the second examination. Patients in children's hospitals rely on assessments by pediatric specialists who understand the unique needs of children and their families. The approach to caring for children is very different and likely more family centered. These issues are further addressed in the full guideline and we encourage readers to review the entire document published in Critical Care Medicine and Pediatrics.[2,5]

Declaring brain death in children is complicated and should be undertaken by physicians who are adequately trained in the complexities involved in this important determination. We agree more research is needed to address some of the other issues raised in the editorial, and we again thank Drs Wijdicks and Smith for their opinion.

Potential Conflicts of Interest

Nothing to report.

[1]Departments of Anesthesiology (Section on Pediatric Critical Care) and Pediatrics, Wake Forest School of Medicine, Winston-Salem, NC, [2]Department of Pediatrics (Division of Child Neurology) and [3]Division of Pediatric Critical Care, Loma Linda University School of Medicine, Loma Linda, CA, and [4]Department of Pediatrics, University of Nebraska College of Medicine, Omaha, NE

References

1. Wijdicks EF, Smith WS. Brain death in children: why does it have to be so complicated? Ann Neurol 2012;71:442–443.
2. Nakagawa TA, Ashwal S, Mathur M, et al. Guidelines for the determination of brain death in infants and children: an update of the 1987 Task Force recommendations. Crit Care Med 2011;39:2139–2155.
3. Wijdicks EF, Varelas PN, Gronseth GS, et al. Evidence-based guideline update: determining brain death in adults: report of the Quality Standards Subcommittee of the American Academy of Neurology. Neurology 2010;74:1911–1918.
4. Fackler J, Goldstein B. Pediatric brain death. Crit Care Med 2011; 39;2197–2198.
5. Clinical report - Guidelines for the Determination of Brain Death in Infants and Children. An Update of the 1987 Task Force Recommendations. Nakagawa TA, Ashwal, SA, Mathur M, Mysore M., and the Committee for Brain Death in Infants and Children. Pediatrics. 2011;128:3 e720-e740. doi: 10.1542/peds.2011-1511.

DOI: 10.1002/ana.23623

CLINICAL GENETICS An International Journal of Genetics, Molecular and Personalized Medicine

Clin Genet 2013: 83: 135–144
Printed in Singapore. All rights reserved

CLINICAL GENETICS
doi: 10.1111/j.1399-0004.2012.01885.x

Original Article

Exome sequencing in a family with an X-linked lethal malformation syndrome: clinical consequences of hemizygous truncating *OFD1* mutations in male patients

Tsurusaki Y, Kosho T, Hatasaki K, Narumi Y, Wakui K, Fukushima Y, Doi H, Saitsu H, Miyake N, Matsumoto N. Exome sequencing in a family with an X-linked lethal malformation syndrome: clinical consequences of hemizygous truncating *OFD1* mutations in male patients.
Clin Genet 2013: 83: 135–144. © John Wiley & Sons A/S. Published by Blackwell Publishing Ltd, 2012

Oral-facial-digital syndrome type 1 (OFD1; OMIM #311200) is an X-linked dominant disorder, caused by heterozygous mutations in the *OFD1* gene and characterized by facial anomalies, abnormalities in oral tissues, digits, brain, and kidney; and male lethality in the first or second trimester pregnancy. We encountered a family with three affected male neonates having an 'unclassified' X-linked lethal congenital malformation syndrome. Exome sequencing of entire transcripts of the whole X chromosome has identified a novel splicing mutation (c.2388+1G > C) in intron 17 of *OFD1*, resulting in a premature stop codon at amino acid position 796. The affected males manifested severe multisystem complications in addition to the cardinal features of OFD1 and the carrier female showed only subtle features of OFD1. The present patients and the previously reported male patients from four families (clinical OFD1; Simpson-Golabi-Behmel syndrome, type 2 with an *OFD1* mutation; Joubert syndrome-10 with *OFD1* mutations) would belong to a single syndrome spectrum caused by truncating OFD1 mutations, presenting with craniofacial features (macrocephaly, depressed or broad nasal bridge, and lip abnormalities), postaxial polydactyly, respiratory insufficiency with recurrent respiratory tract infections in survivors, severe mental or developmental retardation, and brain malformations (hypoplasia or agenesis of corpus callosum and/or cerebellar vermis and posterior fossa abnormalities).

Conflict of interest

The authors have no conflict of interest to declare.

Y Tsurusaki[a]*, T Kosho[b]*, K Hatasaki[c], Y Narumi[b], K Wakui[b], Y Fukushima[b], H Doi[a], H Saitsu[a], N Miyake[a] and N Matsumoto[a]

[a]Department of Human Genetics, Yokohama City Graduate School of Medicine, Yokohama, Japan, [b]Department of Medical Genetics, Shinshu University School of Medicine, Matsumoto, Japan, and [c]Department of Pediatrics, Toyama Prefectural Central Hospital, Toyama, Japan

*These authors contributed equally to this work.

Key words: exome sequencing – OFD1 – *OFD1* gene – splicing mutation – X-linked congenital malformation syndrome

Corresponding authors: Tomoki Kosho, MD, Department of Medical Genetics, Shinshu University School of Medicine, 3-1-1 Asahi, Matsumoto, Nagano 390-8621, Japan.
Tel.: +81 263 37 2618;
fax: +81 263 37 2619;
e-mail: ktomoki@shinshu-u.ac.jp
and
Naomichi Matsumoto, MD, PhD, Department of Human Genetics, Yokohama City Graduate School of Medicine, 3-9 Fukuura, Kanazawa-ku, Yokohama 236-0004, Japan.
Tel.: +81 45 787 260;
fax: +81 45 786 5219;
e-mail: naomat@yokohama-cu.ac.jp

Received 14 January 2012, revised and accepted for publication 26 March 2012

Oral-facial-digital syndrome type 1 (OFD1; OMIM #311200), originally described by Papillon-Leage and Psaume (1) and further delineated by Gorlin and Psaume (2), is an X-linked dominant developmental disorder with an estimated prevalence of 1:50,000, caused by mutations in the *OFD1* gene (OMIM #300170) (3–5). The disorder is characterized by facial anomalies and abnormalities in oral tissues, digits, brain and kidney (5). Almost all affected individuals with OFD1 are female, with highly variable expression, possibly resulting from random X inactivation (6). Affected males are generally lost in the first or second trimester of pregnancy (4). To date, only one liveborn male case with clinically definite OFD1 and a normal karyotype has been reported; the patient was born at 34 weeks of gestation and died 21 h after birth due to heart failure (7). In this report, we describe a family with three affected male neonates having an 'unclassified' X-linked lethal congenital malformation syndrome. Exome sequencing of entire transcripts of the whole X chromosome has successfully identified a causative splicing mutation in *OFD1*.

Subjects and methods

Clinical report

II-2, a 22-year-old woman, was referred to our clinic for genetic counseling (Fig. 1). Her deceased brother (II-4) had severe multiple congenital abnormalities. She had two sons (III-1 and III-5) with similar congenital abnormalities and a healthy boy (III-3) as well as two miscarriages (III-2, artificial; III-4, spontaneous). During genetic counseling and molecular investigations, she had another healthy boy (III-5). After identification of a heterozygous *OFD1* mutation, she was examined for features of OFD1. Only a few accessory frenulae and irregular teeth with no facial anomalies or tongue abnormalities were observed (Fig. 2a–e). A radiograph of her hands showed no abnormalities (Fig. 2f) and an abdominal ultrasonography detected no cysts in the kidneys, liver, or pancreas (data not shown). I-2, allegedly, had no apparent malformations or complications including renal diseases.

II-4 was born by caesarean section because of placental abruption at 33 weeks of gestation. Pregnancy was complicated by polyhydramnios. Apgar score was 3 at 1 min. His birth weight was 2056 g (+0 SD), length was 45.0 cm (+0.5 SD), and occipitofrontal circumference (OFC) was 34.0 cm (+2.0 SD). He manifested severe respiratory insufficiency and was transferred to a neonatal intensive care unit (NICU). His craniofacial features included a prominent forehead, a large fontanelle (5 × 5 cm), a low posterior hairline, microphthalmia, hypertelorism, short palpebral fissures, depressed nasal bridge, low-set ears, a small cleft lip and a soft cleft palate, narrowing of the tip of the tongue, and a hypoplastic gum (Fig. 2g). Additional physical features included redundant neck skin, postaxial polydactyly of the left hand (Fig. 2h), wide halluces (Fig. 2i), micropenis, and left cryptorchidism.

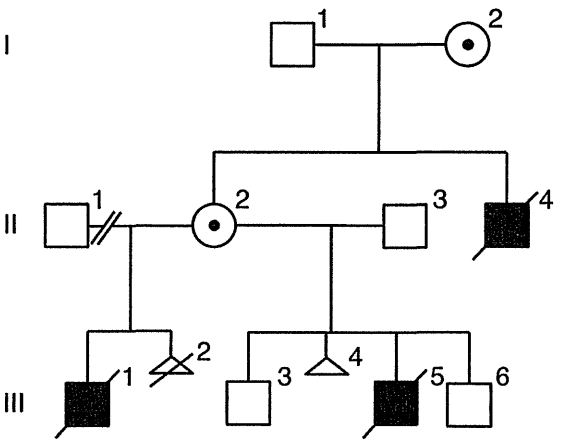

Fig. 1. Familial pedigree.

Ultrasonography revealed hypoplastic gyri, an atrial septal defect, and patent ductus arteriosus. Ophthalmological examination detected microcornea and retinal detachment. Intubation was impossible because of laryngeal anomalies and the patient died 11 h after birth. Additional autopsy findings included partial atelectasis and bilateral hydroureters.

III-1 was delivered by emergency caesarean section at 39 weeks of gestation. Pregnancy was complicated by polyhydramnios and intrauterine growth retardation, with moderate macrocephaly. His birth weight was 3064 g (+0.1 SD). He was admitted to a NICU because of respiratory insufficiency, and received mechanical ventilation. His craniofacial features included microphthalmia, hypertelorism, short palpebral fissures, epicanthus, low-set ears, and a cleft lip and palate. Additional physical features included bilateral polydactyly of hands (postaxial) and feet (preaxial), and an ectopic urethral opening. Ultrasonography revealed hydrocephalus, agenesis of the corpus callosum and cerebellar vermis, and a complete atrioventricular septal defect. Ophthalmological examination detected persistent pupillary membrane and optic disc coloboma. G-banded chromosomes were normal (46,XY). The patient died at age 14 days due to heart failure.

III-5 was delivered by caesarean section at 32 weeks of gestation. Pregnancy was complicated by polyhydramnios, intrauterine growth retardation, and congenital heart defects. His birth weight was 1704 g (−0.2 SD), length was 40.0 cm (−0.8 SD), and OFC was 33.3 cm (+2.0 SD). He was admitted to a NICU because of respiratory insufficiency, and received mechanical ventilation. His craniofacial features included a prominent forehead, hypertelorism, dysplastic ears, a small cleft lip, and a soft cleft palate (Fig. 2j,k). Ultrasonography revealed hydrocephalus with Dandy-Walker malformation and hypoplastic left heart syndrome. G-banded chromosomes were normal (46,XY). The patient died 1 day after birth. Additional autopsy findings included agenesis of the cerebellar vermis (Fig. 2l), enlargement of the fourth ventricle and aqueduct, anomalous positioning of the esophagus, mild

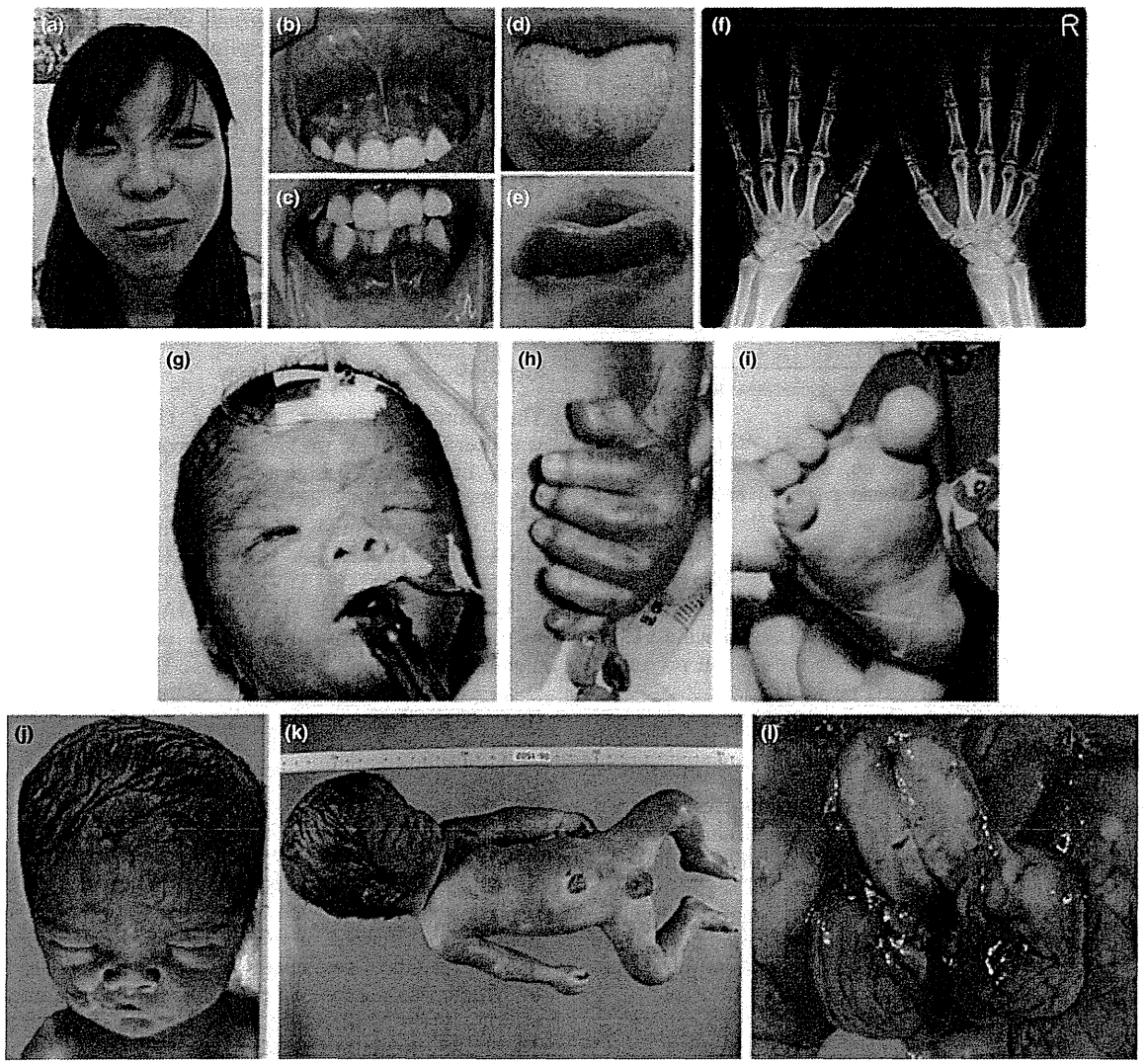

Fig. 2. Clinical photographs of II-2 (**a–f**), II-4 (**g–i**), and III-5 (**j–l**).

pulmonary congestion, and insufficient lobulation of the right lung.

The three affected male neonates, having strikingly similar clinical manifestations (Table 1), are considered to have had a congenital malformation syndrome with X-linked inheritance. Array-CGH analysis using 4200 BAC clones identified no pathologic genomic copy number abnormalities. Direct sequencing of *MID*, performed because of a partial similarity to these neonates' syndrome to X-linked Opitz-G/BBB syndrome (OMIM #300000) (8), revealed no mutation.

Library preparation

Genomic DNA for II-2, II-3, III-3, and III-6 was extracted from peripheral blood using the Gentra PureGene Blood Kit (QIAGEN, Hilden, Germany), and genomic DNA for III-5 was extracted from the preserved dried umbilical cord using the DNeasy Blood & Tissue Kit (QIAGEN). Three micrograms of high-quality (absorbance at 260 nm/absorbance at 280 nm: 1.8–2.0) genomic DNA from II-2 was fragmented using the Covaris model S2 system (Covaris, Woburn, MA). The target peak size was 150 bp. After the size of sheared DNA was checked using an Agilent 2100 Bioanalyzer (Agilent Technologies, Santa Clara, CA), adapter sequences were ligated to the ends of DNA fragments, and amplified according to the manufacturer's protocol (Agilent Technologies).

Exome capture and next-generation sequencing

Library DNA was hybridized for 24 h at 65°C using the SureSelect Human X Chromosome Demo Kit (Agilent Technologies). Captured DNA was diluted to a concentration of 8 pM and sequenced on a Genome Analyzer IIx (Illumina, San Diego, CA) with 76-bp paired-end reads. We used only one of the eight lanes in the flow